Light Higgsinos at LHC with Right Sneutrino LSP

Juhi Dutta

Harish Chandra Research Institute, Allahabad, India

December 11, 2018

JHEP 1806 (2018) 042

with A. Chatterjee, S.K. Rai

The Model

- We focus on an extended version of the Minimal supersymmetric standard model (MSSM) with right handed neutrino superfield ($\hat{N}$) with Majorana mass parameter M_R.
- Superpotential:

$$\mathcal{W} \supset \mathcal{W}_{\mathcal{MSSM}} + y_\nu \hat{L} \hat{H}_u \hat{N}^c + \frac{1}{2} M_R \hat{N}^c \hat{N}^c$$

- The soft supersymmetric scalar potential has new terms:

$$\mathcal{V}^{soft} \supset \mathcal{V}^{soft}_{MSSM} + m_R^2 |\widetilde{N}|^2 + \frac{1}{2} B_M \widetilde{N}^c \widetilde{N}^c + (T_\nu \widetilde{L} H_u \widetilde{N}^c + \text{ h.c.})$$

Sneutrino Sector

- In the CP basis, the sneutrino mass matrix is:

$$\mathcal{M}^{j\ 2} = \begin{pmatrix} m^2_{LL} & m^{j2}_{LR} \\ m^{j\ 2}_{LR} & m^{j\ 2}_{RR} \end{pmatrix},$$

where,

$$\begin{aligned} m^2_{LL} &= m^2_L + \frac{1}{2} m^2_Z \cos 2\beta + m^2_D, \\ m^{j\ 2}_{LR} &= (T_\nu \pm y_\nu M_R) v \sin\beta - \mu m_D \cot\beta, \\ m^{j\ 2}_{RR} &= m^2_R + m^2_D + M^2_R \pm B_M, \end{aligned} \tag{1}$$

j = even, odd states and $m_D = y_\nu v_u$, the Dirac mass obtained by SM neutrinos after electroweak symmetry breaking, i.e, $< H^0_u >= v_u$.

- Diagonalizing the mass matrix, the mass eigenvalues are given by:

$$m^{j\,2}_{1,2} = \frac{1}{2}\left(m^2_{LL} + m^{j\,2}_{RR} \pm \sqrt{(m^2_{LL} - m^{j\,2}_{RR})^2 + 4m^{j\,4}_{LR}}\right). \quad (2)$$

- Presence of non-zero B_M generates a mass split between the sneutrino mass eigenstates.
- Left-right mixing angle θ in the sneutrino sector,

$$\sin 2\theta^j = \frac{(T_\nu \pm y_\nu M_R)v \sin\beta - \mu m_D \cot\beta}{m^{j2}_2 - m^{j2}_1}, \quad (3)$$

- Choice of $T_\nu \sim \mathcal{O}(1)\mathrm{GeV}$ leads to increased mixing in the sneutrino sector.
- Radiative contribution to neutrino mass arise in presence of non-zero B_M, T_ν from sneutrino-gaugino loops.

Constraints on $B_M - T_\nu$ parameter space.

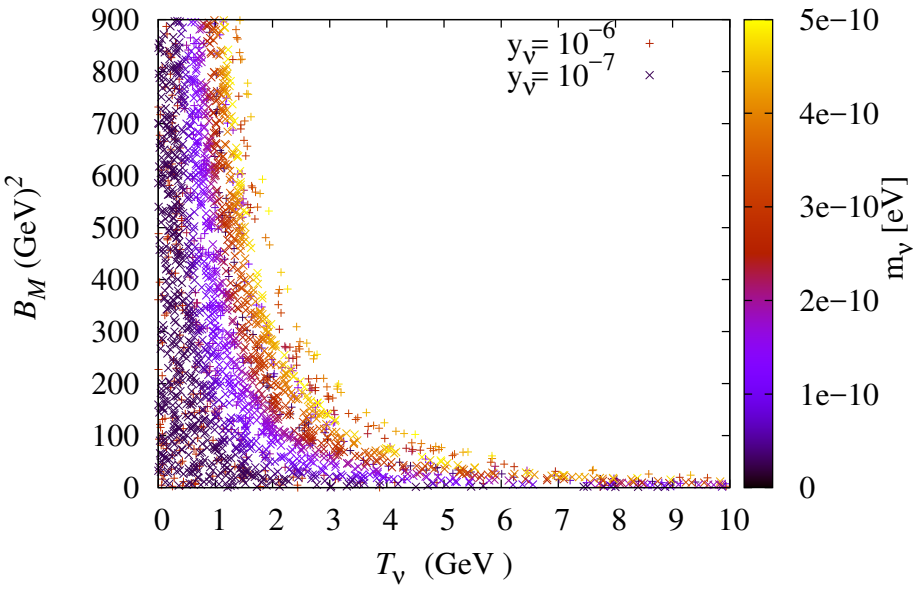

Figure : Allowed regions of B_M and T_ν plane for $M_1 = 1.5$ TeV, $M_2 = 1.8$ TeV and gaugino fraction $\sim \mathcal{O}(10^{-2})$. The colored palette denotes the mass of the heaviest neutrino. We consider $y_\nu \in \{10^{-6}, 10^{-7}\}$, $\mu = 300$ GeV, $M_3 = 2$ TeV, $M_{Q_3} = 1.5$ TeV, $T_t = 2.9$ TeV, $M_{L_{1/2}} = 600$ GeV, $m_{\tilde{\nu}}^{soft} = 100$ GeV and $M_A = 2.5$ TeV.

Large B_M and large T_ν stringently constrained from neutrino mass.

Electroweakino sector

- Naturalness $\Longrightarrow$ low μ $\Longrightarrow$ low-lying compressed higgsinos
- In the limit $M_1, M_2 \gg |\mu|$,

$$m_{\widetilde{\chi}_1^{\pm}} = |\mu|(1 - \frac{M_W^2 \sin 2\beta}{\mu M_2}) + \mathcal{O}({M_2}^{-2}) + \text{rad. corr.}$$

$$m_{\widetilde{\chi}_{a,s}^0} = \pm\mu - \frac{M_Z^2}{2}(1 \pm \sin 2\beta)(\frac{\sin\theta_W^2}{M_1} + \frac{\cos\theta_W^2}{M_2}) + \text{rad. corr.}$$

where the subscripts s(a) denote symmetric (anti-symmetric) higgsino states respectively (M.Drees et.al, hep-ph/9701219).

Effect of M_1, M_2 on the higgsino sector

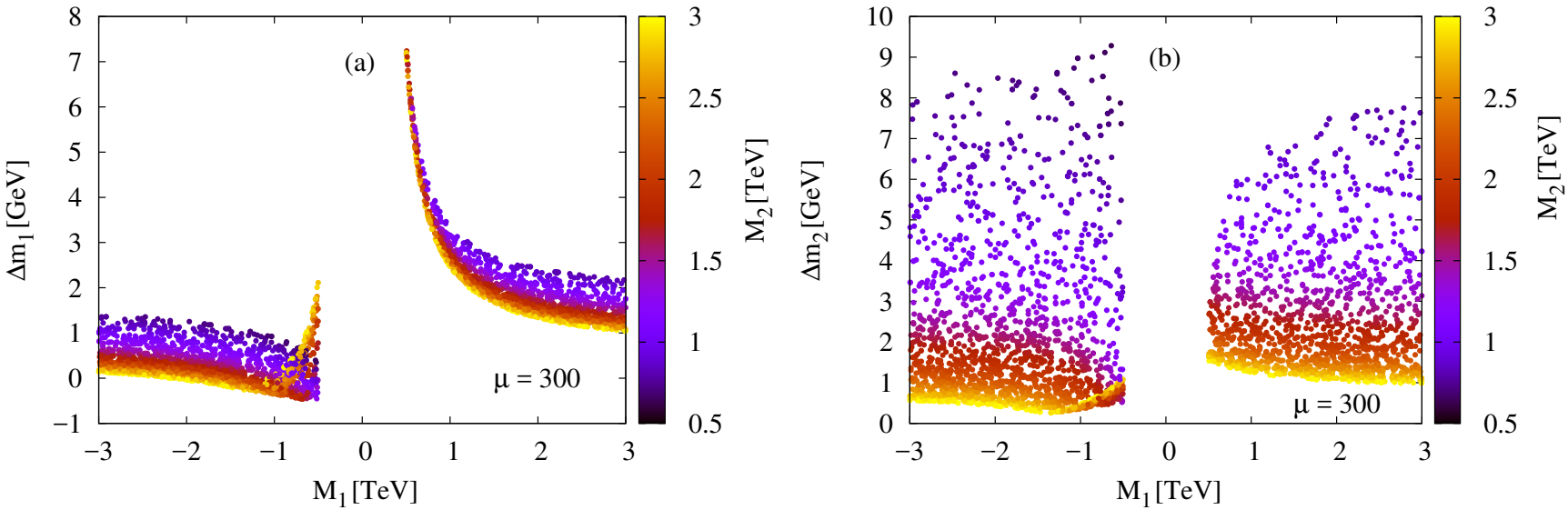

Figure : The left (right) panel shows the variation of the mass difference $\Delta m_1 = m_{\tilde{\chi}_1^\pm} - m_{\tilde{\chi}_1^0}$ ($\Delta m_2 = m_{\tilde{\chi}_2^0} - m_{\tilde{\chi}_1^\pm}$) between $\tilde{\chi}_1^\pm$ and $\tilde{\chi}_1^0$ [$\tilde{\chi}_2^0$] for $\tan\beta = 5$ with respect to M_1, with M_2 on the palette. The other relevant parameters are $\mu = 300\text{GeV}$, $T_t = 2.9$ TeV, $M_{Q_3} = 1.3$ TeV, $M_{U_3} = 2$ TeV and $M_3 = 2$ TeV.

Spectra of interest

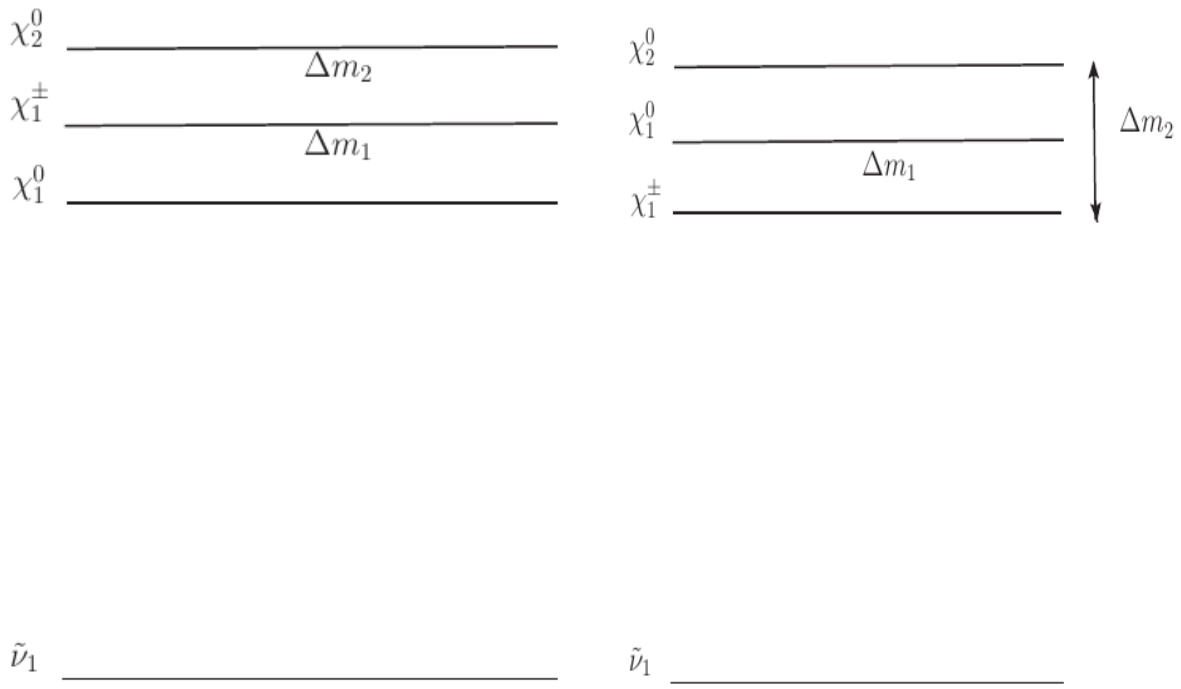

Figure : Schematic description of the mass spectrum with $|M_1|, M_2 \gg |\mu|$, and $m_{\tilde{\nu}_1} < |\mu|$. Here $|m_{\tilde{\chi}_2^0}| - m_{\tilde{\chi}_1^\pm} = \Delta m_2$, $m_{\tilde{\chi}_1^\pm} - |m_{\tilde{\chi}_1^0}| = \Delta m_1$. Here, $M_1, M_2 \sim \mathcal{O}(1)$TeV.

Decays of higgsinos

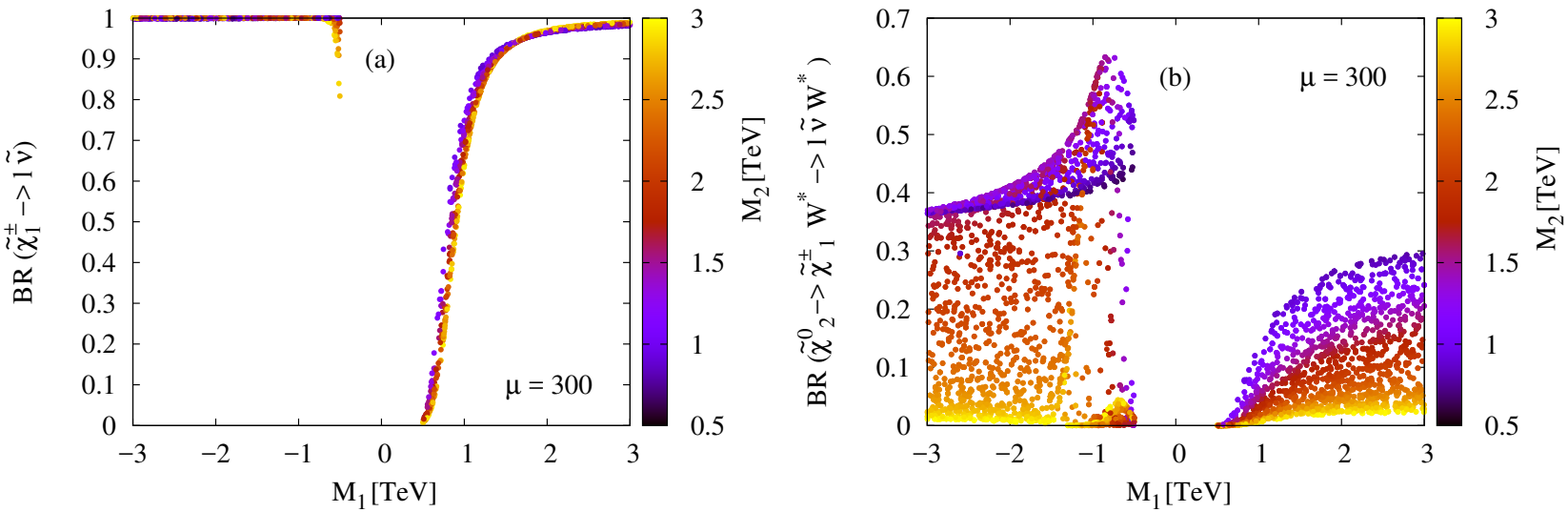

Figure : Variation of the leptonic branching ratios of $\widetilde{\chi}_1^{\pm} \to l\widetilde{\nu}$ and $\widetilde{\chi}_2^0 \to l\widetilde{\nu}W^*$ against the bino soft mass parameter, M_1 for the Higgsino mass parameter, $\mu = 300$ GeV. The wino soft mass parameter M_2 is shown in the palette. $T_\nu > 10^{-2}$ GeV for prompt decay of $\widetilde{\chi}_1^{\pm}$.

Presence of sneutrino LSP opens up new leptonic channels for the compressed higgsinos.

Right sneutrino as Dark Matter

For $y_\nu \sim 10^{-6} - 10^{-7}$, co-annihilation of DM with the higgsinos give correct, Ωh^2_{DM}. Further, m_{DM} at higgs or heavy higgs resonance also lead to correct relic density.

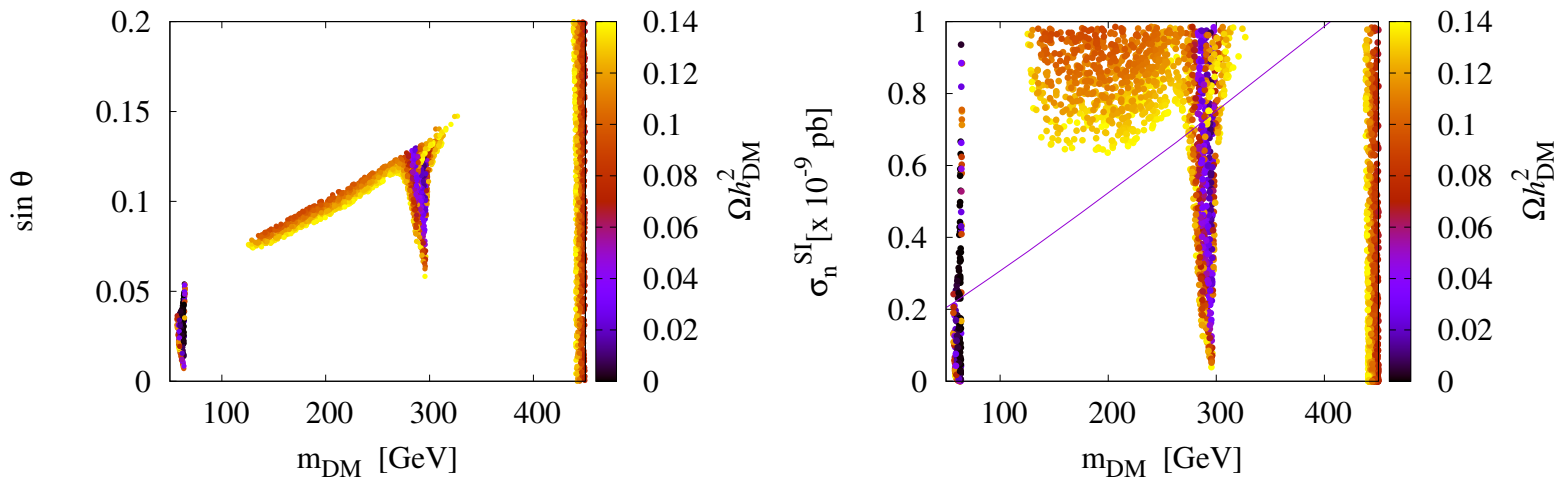

Figure : Dependence of the relic abundance of $\tilde{\nu}_1$ on its mass vs. left-sneutrino fraction and direct detection constraint from XENON-1T for $|\mu| = 450$ GeV, $M_A = 600$ GeV and rest as before.

Collider Signatures

SUSY signals: $\widetilde{\chi}_1^0\widetilde{\chi}_2^0$, $\widetilde{\chi}_1^\pm\widetilde{\chi}_1^0$, $\widetilde{\chi}_1^\pm\widetilde{\chi}_1^\pm$, $\widetilde{\chi}_1^+\widetilde{\chi}_1^-$

- $1\ l + \leq 1\ j + \not{E}_T$ (Mono-lepton)
- $2\ l\ (\ l^+l^-) + 0\ j + \not{E}_T$ (Opposite-sign dilepton)
- $2\ l\ (\ l^\pm l^\pm) + 0\ j + \not{E}_T$ (Same sign dilepton)

- Utilising low jet multiplicity(n_{jet}), transverse mass M_T, missing transverse energy ($\not{E}_T$), M_{T_2} to remove dominant SM backgrounds: W+j, $t\bar{t}$,Drell Yan, WZ.
- $t\bar{t}$ backgrounds reduced using b-veto, $n_{jet} \leq 1$, $M_T(l, \not{E}_T)$ and $\not{E}_T > 100$ GeV for mono-lepton. For dilepton, $n_{jet} = 0$ and M_{T_2} cut further reduces $t\bar{t}$ significantly.

Results

- Monolepton channel with low hadronic activity is the best channel for large $\Delta M = (m_{NLSP} - m_{LSP})(> 50)$ GeV and moderate $BR(\widetilde{\chi}_1^{\pm} \to l\widetilde{\nu}) \sim 0.1 - 0.3$.
- For large $BR(\widetilde{\chi}_1^{\pm} \to l\widetilde{\nu})(\sim 1.0) \implies$ opposite sign dilepton channels most favoured.
- Same sign dileptons $\implies$ strong confirmatory channels for a sneutrino LSP over $\widetilde{\chi}_1^0$ LSP.

Conclusions

- Viability of low μ parameter, hence a light higgsino sector, depends crucially on the choice of M_1, M_2.
- Presence of sneutrino LSP open up visible leptonic channels for observing the compressed higgsino sector.
- For $\mu = 300 - 500$ GeV leptonic channels upto two leptons with low hadronic activity and missing energy observable at 13 TeV high-luminosity LHC.

Thank You

Backup Slides

General constraints

- The light higgs mass, $122 < m_h(GeV) < 128$.
- LEP constraint on the lightest chargino, $m_{\widetilde{\chi}_1^{\pm}} > 103.5 GeV$
- The light sneutrino can contribute to the non-standard decay channels of higgs and /or Z boson. Hence, we choose $m_{\widetilde{\nu}} > 65$ GeV to avoid any contribution.

Benchmarks

- **Region A**: $M_1 > 0$, $M_2 > 0$ and $\mu > 0$, with $\widetilde{\chi}_1^0$ as NLSP (**BP1**).
- **Region B**: $M_1 > 0$, $M_2 > 0$ and $\mu < 0$, with $\widetilde{\chi}_1^0$ as NLSP (**BP2-a** and **BP2−b**).
- **Region C**: $M_1 < 0$, $M_2 > 0$ and $\mu > 0$, with $\widetilde{\chi}_1^{\pm}$ as NLSP (**BP3** and **BP4**).

Benchmarks

Parameters	BP1	BP2−a	BP2−b	BP3	BP4
μ	300	-500	-300	300	400
$\tan\beta$	5	5	10	5	6.1
M_1	1500	1500	2000	-860	-1150
M_2	1800	1800	1000	2500	2500
M_A	2500	803.2	2500	2500	2500
M_R	100	100	100	100	100
B_M (GeV^2)	10^{-3}	10.7	143	10^{-3}	10^{-3}
$m_{\widetilde{\nu}}$	100	404	245	245	316.2
$Y_\nu(\times 10^{-7})$	1	10	1	1	1
T_ν	0.02	140	0.8	4.0	0.06
$m_{\widetilde{\chi}_1^\pm}$	303.6	510.9	307.5	305.4	407.2
$m_{\widetilde{\chi}_1^0}$	301.7	508.4	303.5	305.5	407.3
$m_{\widetilde{\chi}_2^0}$	305.8	512.2	311.5	305.8	407.5
$m_{\widetilde{\nu}_L}$	372.4	624.5	611.7	612.9	613.5
$m_{\widetilde{\nu}_R}$	141.4	412.2	264.1	264.6	331.7
Δm_1	1.9	2.5	4.0	-0.1	-0.1
Δm_2	2.2	3.8	4.0	0.4	0.2
ΔM	162.2	96.2	43	40.9	75.5
$\sin\theta^j(\times 10^{-2})$	0.002	10.9	0.046	0.224	0.004
$BR(\widetilde{\chi}_1^\pm \to l\,\widetilde{\nu})$	0.13	1.00	0.34	1.0	1.0
$BR(\widetilde{\chi}_2^0 \to W^{\mp *}\,\widetilde{\chi}_1^\pm \to l\widetilde{\nu}\,W^{*\mp})$	0.015	0.0	0.031	0.0001	0.10

Prompt decays of Higgsinos in presence of LSP

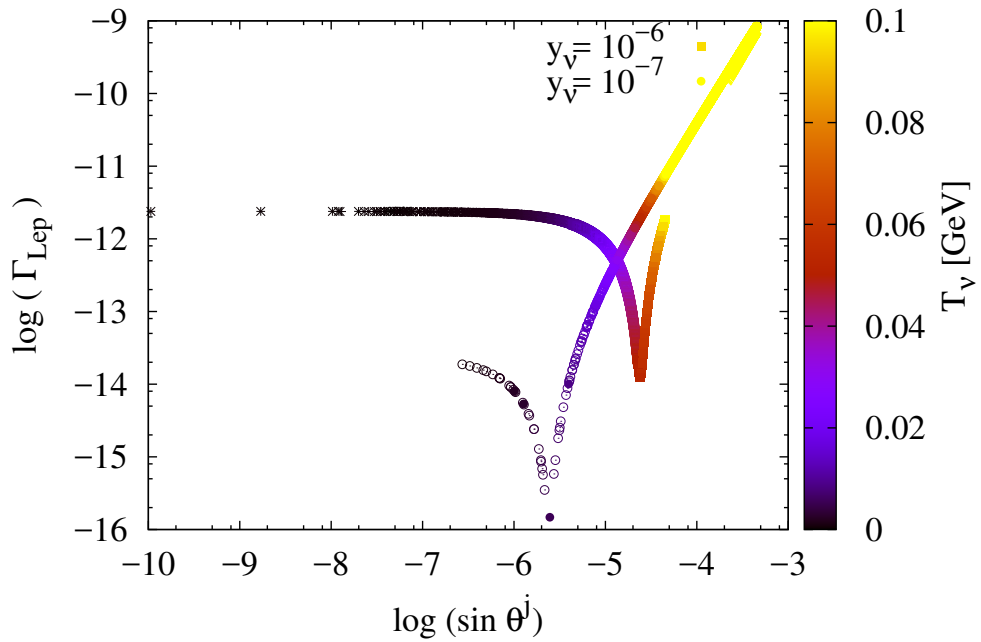

Figure : Variation of the partial decay width of $\widetilde{\chi}_1^{\pm} \to l\,\widetilde{\nu}$ versus $\sin(\theta^j)$ in logarithmic scale for $M_1 = -1.5$ TeV, $M_2 = 1.8$ TeV and gaugino fraction $\sim \mathcal{O}(10^{-2})$. Further, $M_R = 100$ GeV, $M_{L_{1/2}} = 600$ GeV, $m_{\tilde{\nu}}^{soft} = 100$ GeV, $\mu = 300$ GeV and $\tan\beta = 5$. The colored palette corresponds to T_ν, the soft left-right mixing parameter in the sneutrino sector.

$T_\nu > 10^{-2}$ for prompt decay of $\widetilde{\chi}_1^{\pm}$.

Contribution to the light Majorana neutrino mass

- Active neutrinos have masses $m_\nu \simeq \frac{y_\nu^2 v_u^2}{M_R}$, as in Type 1 seesaw mechanism. For $M_R \sim \mathcal{O}(100)\,GeV$, $y_\nu = 10^{-6} - 10^{-7}$ to fit $m_\nu \sim \mathcal{O}(0.1)$eV.
- Radiative corrections to neutrinos from sneutrino-neutralino loops in presence of left-right sneutrino mixing.
- Contribution proportional to mass splitting between CP even and CP odd sneutrino, i.e, B_M parameter for significant L-R mixing controlled by T_ν. (Y.Grossman, et. al, hep-ph/9702421)

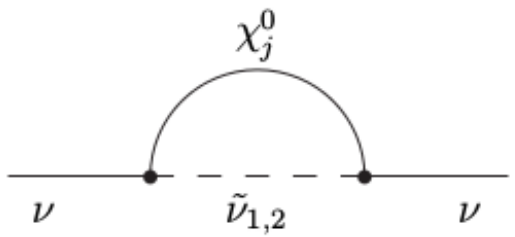

Figure : Schematic diagram showing the leading one-loop contribution to the light neutrino mass.

Radiative contribution to neutrino mass

- Existence of a sneutrino mass splitting generates contribution to neutrino mass.
- The radiative contribution to neutrino mass arising from $\widetilde{\chi}_i^0$-$\widetilde{\nu}$ loop is:

$$m_\nu^{(1)} = \frac{g^2 \Delta m_{\widetilde{\nu}}}{32\pi^2 cos^2\theta_W} \Sigma_j f(y_j) |Z_{jZ}|^2 \tag{4}$$

$$\text{where } f(y_j) = \sqrt{y_j} \frac{[y_j - 1 - ln(y_j)]}{(1-y_j)^2},\ y_j = \frac{m^2_{\widetilde{\nu}}}{m^2_{\widetilde{\chi}_j^0}},$$

$$Z_{jZ} = Z_{j2} cos\theta_W - Zj_1 sin\theta_W .$$

Electroweak Naturalness

After electroweak symmetry breaking,

$$\frac{M_Z^2}{2} = \frac{m_{H_d}^2 - (m_{H_u}^2)\tan\beta^2}{\tan\beta^2 - 1} - \mu^2, \tag{5}$$

where $m_{H_d}^2$ and $m_{H_u}^2$ are the soft squared mass matrix for up and down type Higgs doublets.

- Electroweak scale fine tuning Δ_{EW} (Baer, et. al, arXiv: 1306.2926) as a measure of naturalness, i.e $\mu <= 300$ GeV, $\Delta_{EW} \leq 30$.

$$\Delta_{EW} = \frac{max(|\frac{-m_{H_u}^2 \tan^2\beta}{\tan^2\beta - 1}|, ..., |-\mu^2|)}{M_Z^2/2}$$

- Focus on low μ parameter values and hence a light higgsino sector.
- Stops and gluinos may be kept heavy upto 1.5 and 3-4 TeV respectively.

Simulation details

- SUSY Signal: $\widetilde{\chi}_1^+\widetilde{\chi}_1^-$, $\widetilde{\chi}_2^0\widetilde{\chi}_1^0$, $\widetilde{\chi}_1^0\widetilde{\chi}_1^\pm$, $\widetilde{\chi}_2^0\widetilde{\chi}_1^\pm$
- UFO file from SARAH
- Spectrum Generator: SARAH-SPheno
- Madgraph5 $\rightarrow$ Pythia6 $\rightarrow$ Delphes-v3 for event generation,showering and detector simulation.
- MLM matching performed for SM background with QCUT values 20 GeV.
- Benchmarks passed through Checkmate and Madanalysis5 for constraints from recent LHC search results with low hadronic activity.

Primary Selection Cuts and Kinematic Observables

- We select leptons (e, μ) satisfying $p_T > 10$ GeV and $|\eta| < 2.5$.
- We choose photons with $p_T > 10$ GeV and $|\eta| < 2.5$.
- Reconstructed jets are identified as signal jets if they have $p_T > 40$ GeV and $|\eta| < 2.5$.
- Reconstructed b-tagged jets are identified with $p_T >$40 GeV and $|\eta| < 2.5$.
- Jets and leptons are isolated such that $\Delta R_{lj} > 0.4$ and $\Delta R_{ll} > 0.2$.

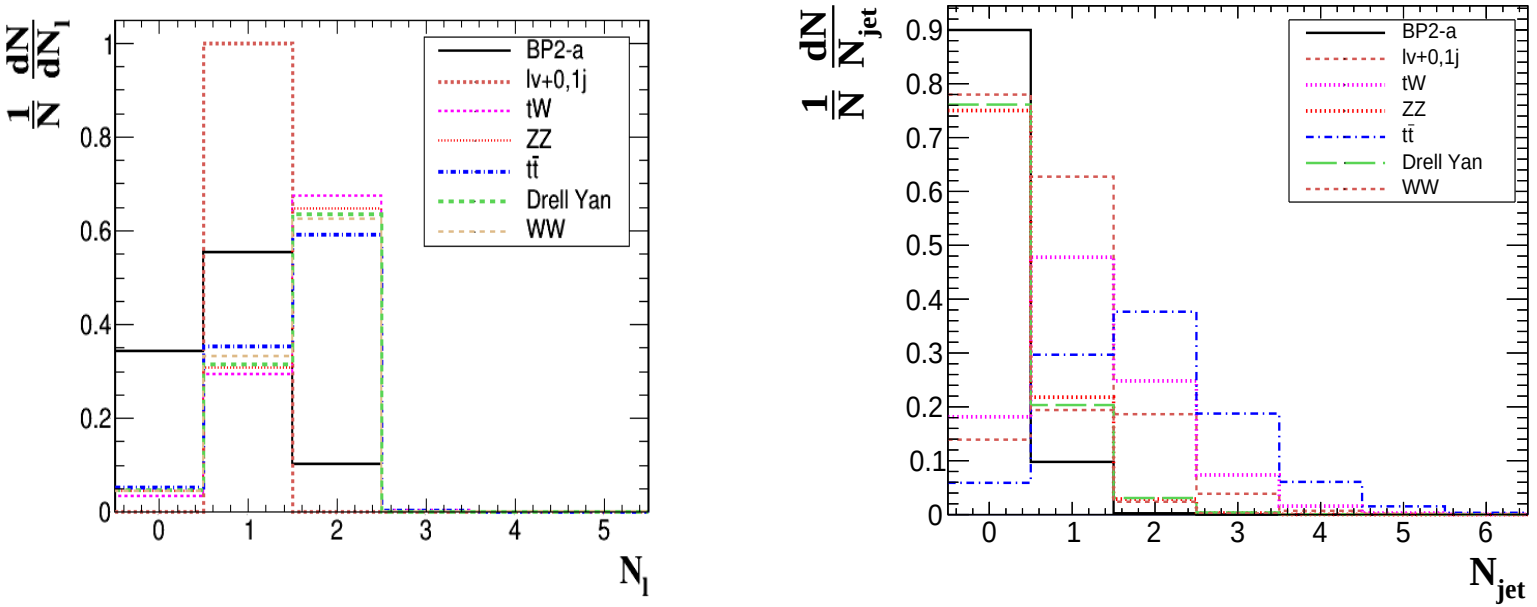

Figure : Normalized distributions for lepton and jet multiplicity for benchmark **BP2** and dominant SM backgrounds channels. respectively.

Focus on low hadronic activity to reduce SM backgrounds.

Important kinematic variable for monolepton final state

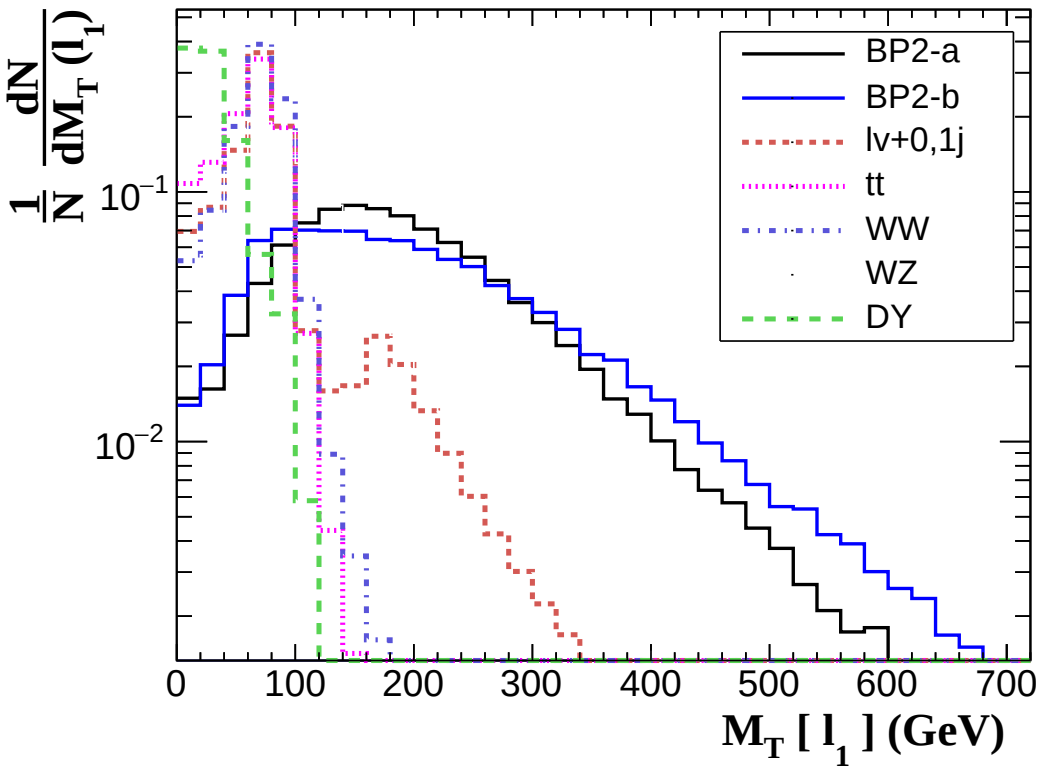

Figure : Normalized distribution for $M_T(l_1) = M_T(l, \not{E}_T) = \sqrt{2p_T(l)\not{E}_T(1-\cos(\Delta\phi))}$, the transverse mass of the leading lepton for SUSY signal **BP2 – a** and **BP2 – b** against the dominant SM backgrounds after selection of the mono-lepton final state.

Required Luminosities for Mono-lepton Channel

Signal	$\mathcal{L}_{3\sigma}$ (fb^{-1})	$\mathcal{L}_{5\sigma}$(fb^{-1})
BP1	254	704
BP2-a	1384	3485
BP2-b	106	293
BP3	613	1701
BP4	448	1245

Table : Required luminosities for discovery of mono lepton final states with missing energy at $\sqrt{s} = 13$ TeV LHC.

Monolepton channel is a good probe for this scenario for most benchmarks. Also pointed out earlier by Kraml, et. al (1503.02960).

Important Kinematic variables for OSDL final state

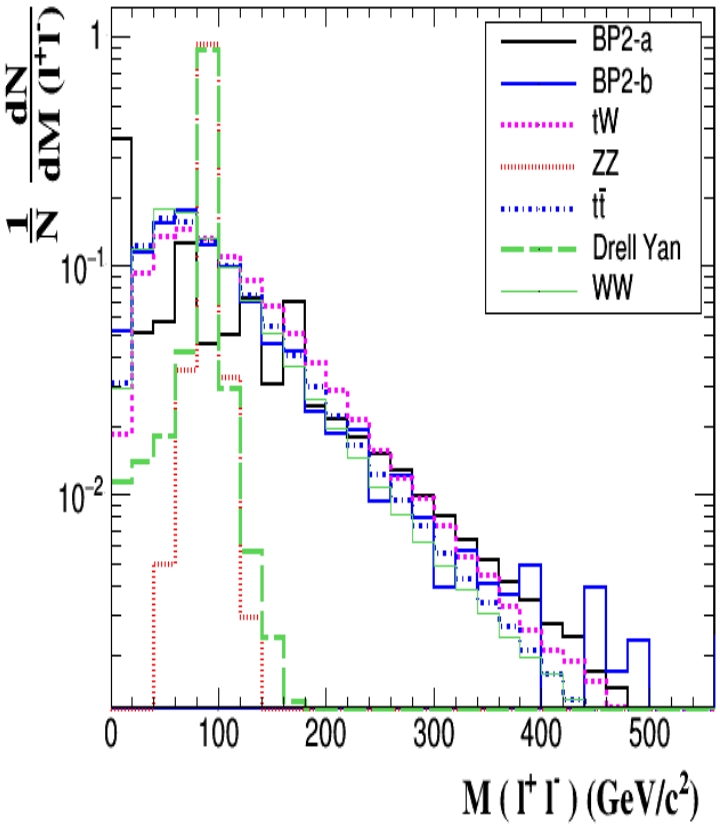

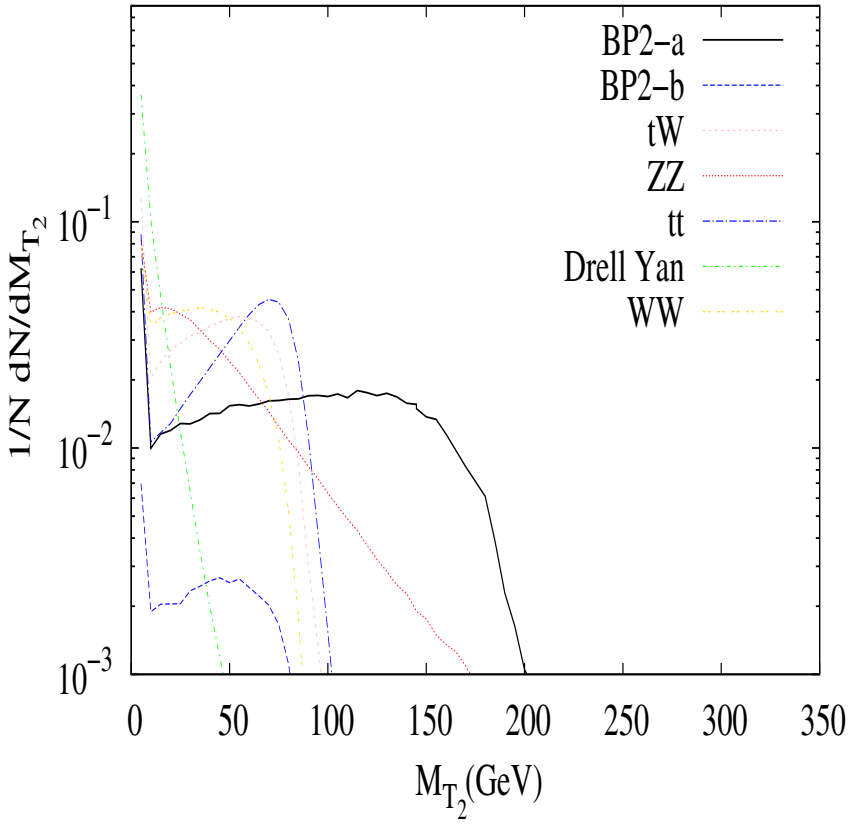

Figure : Normalized distributions of several kinematic variables after selecting the final state with two opposite sign leptons.

Required Luminosities for OSDL channel

Signal	$\mathcal{L}_{3\sigma}$ (fb^{-1})	$\mathcal{L}_{5\sigma}$(fb^{-1})
BP1	568	1576
BP2-a	51	142
BP2-b	1.83×10^4	5.07×10^4
BP3	1035	2875
BP4	160	444

Table : Required luminosities for discovery of opposite sign di-lepton + $\not{E}_T$ final states at $\sqrt{s} = 13$ TeV LHC.

Most favoured channel for large leptonic branching fractions and large mass gap scenarios ($\mathbf{BP2-a}$) whereas suppressed for more compressed scenarios where mono-lepton is a better probe.

Required Luminosities for SSDL channel

Signal	$\mathcal{L}_{3\sigma}$ (fb^{-1})	$\mathcal{L}_{5\sigma}$(fb^{-1})
BP2-b	811	2251
BP4	1052	3845

Table : Required luminosities for discovery of same sign di-lepton final states with missing energy at $\sqrt{s} = 13$ TeV LHC.

Favoured for channels with $\widetilde{\chi}_1^{\pm}$ as NLSP however strongly constrained from current searches. For $\mu = 300$ GeV, SSDL branching $\leq 4\%$ at most. For higher $\mu = 400$ GeV, Br $= 10\%$ but luminosity increases owing to a reduced production cross-section. Still a strong confirmatory channel for discovery.

Monolepton + $\leq 1j + \not{E}_T$

Dominant backgrounds come from:

- $l^{\pm}\nu$+0,1 jets (including contributions from both on-shell and off-shell W boson),
- $t\bar{t}$ (where one of the top quark decays hadronically and the other semi-leptonically).
- Single top quark production ($t(\bar{t})j,\ tW$).
- W^+W^-+ jets ($W \to l\nu,\ W \to jj$).
- $t\bar{t}W$+ jets (when both top quarks decay hadronically and $W \to l\nu$) and
- WZ (with $W \to l\nu,\ Z \to \nu\bar{\nu}/jj$).

Other subdominant contributions come from $t\bar{t}$ (where both top quarks decaying semi-leptonically), Drell Yan process ($l^+l^- + 0, 1j$) and $ZZ, (Z \to l^+l^-, Z \to \nu\bar{\nu}/jj)$ from misidentification.

Kinematic Cuts used

- **M1:** $N_l = 1$, $p_T(l_1) > 25$ **GeV.**
- **M2:** $M_T(l_1) > 150$ **GeV.**
- **M3:** $N_b = 0$
- **M4:** $N_j <= 3$
- **M5:** $\not{E}_T > 100$ **GeV.**
- **M6:** $N_j <= 1$

Opposite sign dileptons + 0j + $\not{E}_T$

Dominant SM contributions to the opposite sign di-lepton signal with missing energy come from:

- $t\bar{t}$
- tW
- Drell Yan
- W^+W^- $(W^+ \to l^+\nu, W^- \to l^-\bar{\nu})$
- ZZ ($Z \to l^+l^-, Z \to jj/\nu\bar{\nu}$)
- WZ+jets $(W \to jj, Z \to l^+l^-)$

Kinematic cuts used

- **D1:** $N_l = 2$ **(opposite sign),** $N_\gamma = 0$
- **D2:** $p_T(l_1) > 20$ **GeV,** $p_T(l_2) > 10$ **GeV**
- **D3:** $M_{l^+l^-} > 10$**,** $76 < M_{l^+l^-} < 106$
- **D4:** $N_b = 0$
- **D5:** $N_j = 0$
- **D6:** $\not{E}_T > 80$ **GeV**
- **D7:** $M_{T_2} > 90$ **GeV**
- **D8:** $\not{E}_T > 100$ **GeV**

Same-sign dilepton + 0 j+$\not{E}_T$

Dominant sources of SM backgrounds :

- WZ
- ZZ
- $W^{\pm}W^{\pm} + jj$
- $t\bar{t}W$
- $t\bar{t}Z$
- WWW

Kinematic cuts used:

- **S1:** $N_l = 2$ **(SS),** $p_T(l_1) > 20$ **GeV,** $p_T(l_2) > 15$ **GeV,** $N_b = 0$
- **S2:** $M_T(l_1) > 100$ **GeV**
- **S3:** $N_j <= 2$
- **S4:** $\not{E}_T > 100$ **GeV**
- **S5:** $N_j = 0$

Relevant current searches at LHC

Final State	ATLAS	CMS
1 l + $\not{E}_T$	1706.4786	CMS-PAS-SUS-16-052
2 l + $\not{E}_T$	ATLAS-CONF-2017-039	CMS-PAS-SUS-17-009(2)
2 same-sign leptons + $\not{E}_T$	-	CMS-SUS-16-039

Table : Leptonic searches at $\sqrt{s} = 13$ TeV LHC with few jets (i,e, $N_j \leq 2$), as relevant for this study.

Forecast from current searches

		Luminosity (in fb^{-1}) for 3σ				
	Ref.	**BP1**	**BP2-a**	**BP2-b**	**BP3**	**BP4**
$l^{\pm}l^{\mp}$+ 0 jet+ $\not{E}_T$	ATLAS-CONF-2017-039	13397	812	-	-	958
$l^{\pm}l^{\mp}$+ 0 jet+ $\not{E}_T$	ATLAS-CONF-2017-039	2191	162	-	-	104
$l^{\pm}l^{\mp}$ + 0 jet+$\not{E}_T$	CMS-PAS-SUS-17-009	-	2223	-	-	385
$l^{\pm}l^{\pm}$ + 0 jet+ $\not{E}_T$	CMS-SUS-16-039	-	-	1997	-	2726
$l^{\pm}l^{\pm}$ + 1 jet+ $\not{E}_T$	CMS-SUS-16-039	-	-	4039	-	4901

Table : Forecast for luminosity for 3σ excess using present experimental searches using 36 fb^{-1} of data at LHC. The blank spaces indicate that the benchmark is not sensitive to the final state analysis. We do not show the forecast from current monoleptonic searches as it gives much weaker sensitivity to our scenario.

Monolepton $+ \leq 1j + \not{E}_T$

	Number of events after cut					
	M1	**M2**	**M3**	**M4**	**M5**	**M6**
BP1	2543	1987	1946	1936	1601	1429
BP2-a	1495	944	922	916	706	611
BP2-b	6252	3194	3128	3118	2462	2215
BP3	1.06×10^4	1664	1614	1601	1138	919
BP4	3919	1793	1751	1740	1258	1074
SM BKG						5.74×10^5

Table : Mono-lepton + missing energy signal final state number of events at 100 fb^{-1} for SUSY signals.

Monolepton $+ \leq 1j + \not{E}_T$

	Number of events after cut					
	M1	**M2**	**M3**	**M4**	**M5**	**M6**
BP1	2543	1987	1946	1936	1601	1429
BP2-a	1495	944	922	916	706	611
BP2-b	6252	3194	3128	3118	2462	2215
BP3	1.06×10^4	1664	1614	1601	1138	919
BP4	3919	1793	1751	1740	1258	1074
SM BKG						5.74×10^5

Table : Mono-lepton + missing energy signal final state number of events at 100 fb^{-1} for SUSY signals.

Background Cut Flow

Background	Number of events after cut					
	M1	**M2**	**M3**	**M4**	**M5**	**M6**
$l\nu + 0, 1j$	1.07×10^7	1.09×10^6	1.08×10^6	1.08×10^5	5.77×10^5	5.49×10^5
Drell Yan	3.52×10^7	3.47×10^4	3.34×10^4	5991	5272	3674
WW	8.04×10^5	5696	5485	5446	1329	1130
WZ	1.56×10^5	2.54×10^4	2.48×10^4	2.20×10^4	1.55×10^4	11523
ZZ	4938	912	900	899	551	492
$t\bar{t}$	2.04×10^6	5.97×10^4	1.79×10^4	1.68×10^4	1.17×10^4	6399
Single top	3.68×10^6	2.05×10^4	8517	8088	2659	1603
Total						5.74×10^5

Table : Mono−lepton + missing energy signal final state number of events at 100 fb^{-1} for SM background.

Opposite-sign dileptons + 0 j + $\not{E}_T$

Signal	Number of events after cut						
	D1	**D2**	**D3**	**D4**	**D5**	**D7**	**D8**
BP1	130	129	112	109	68	22	21
BP2-a	306	271	265	161	108	76	72
BP4	209	298	246	241	153	81	40

Signal	Number of events after cut						
	D1	**D2**	**D3**	**D4**	**D5**	**D6**	
BP2-b	455	452	351	345	230	45	
BP3	2424	2394	1840	1805	1186	189	
Total Bkg						41009	271

Table : Opposite Sign di-lepton + $\not{E}_T$ final state number of events at 100 fb^{-1} for SUSY signals.

	No. of events							
	D1	**D2**	**D3**	**D4**	**D5**	**D6**	**D7**	**D**
DY	1.2×10^8	1.1×10^8	8.9×10^6	8.8×10^6	6.9×10^6	506	293	5
W^+W^-	1.44×10^5	1.4×10^5	1.1×10^5	1.1×10^5	1×10^5	5813	24	1
ZZ	1.7×10^4	1.7×10^4	656	651	504	117	50	4
WZ	6×10^4	6×10^4	5399	5208	1554	92	6	
$t\bar{t}$	6.2×10^5	6.2×10^5	4.9×10^5	1.5×10^5	3.5×10^4	2.6×10^4	132	1
tW	1.8×10^5	1.7×10^5	1.4×10^5	6.8×10^4	3×10^4	8181	114	5
Total						41009		2

Table : Opposite Sign di-lepton + $\not{E}_T$ final state number of events at 100 fb^{-1} for Standard Model backgrounds.

Signal	Number of events after cut:				
	S1	**S2**	**S3**	**S4**	**S5**
BP1	5	5	5	4	2
BP2-a	3	2.5	2.3	1.6	1
BP2-b	32	23	22	15	8
BP3	2	0.5	0.5	0.2	0.1
BP4	30	23	23	13	7
Total background					55

Table : Same sign di-lepton + $\not{E}_T$ final state number of events at 100 fb^{-1} for SUSY signals.

SSDL Background Cut flow

SM Backgrounds	Number of events after cut				
	S1	**S2**	**S3**	**S4**	**S5**
WZ	3856	1053	930	194	39
ZZ	94	6	5	0.5	0.2
WWW	60	29	21	7	0.6
W^+W^+jj	416	175	116	56	2
W^-W^-jj	188	82	57	18	0.5
tW	40	20	19	7	4
$t\bar{t}W$	128	60	30	13	1
$t\bar{t}$	90	65	50	28	8
Total background					55

Table : Same sign di-lepton + $\not{E}_T$ final state number of events at 100 fb^{-1} for SM background.

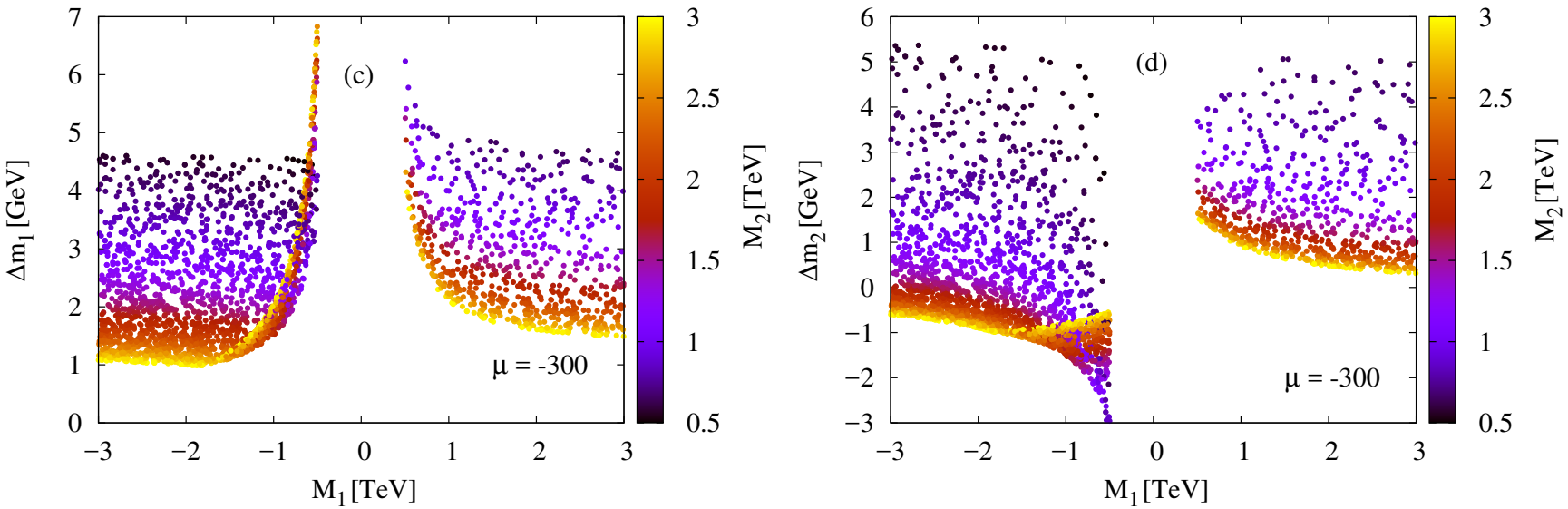

Figure : The left (right) panel shows the variation of the mass difference $\Delta m_1 = m_{\widetilde{\chi}_1^\pm} - m_{\widetilde{\chi}_1^0}$ ($\Delta m_2 = m_{\widetilde{\chi}_2^0} - m_{\widetilde{\chi}_1^\pm}$) between $\tilde{\chi}_1^\pm$ and $\tilde{\chi}_1^0$ [$\tilde{\chi}_2^0$] for $\tan\beta = 5$ with respect to M_1, with M_2 on the palette. Here $\mu = -300$ GeV and other parameters are same as previous figure.

Leptonic Branching of the Higgsinos

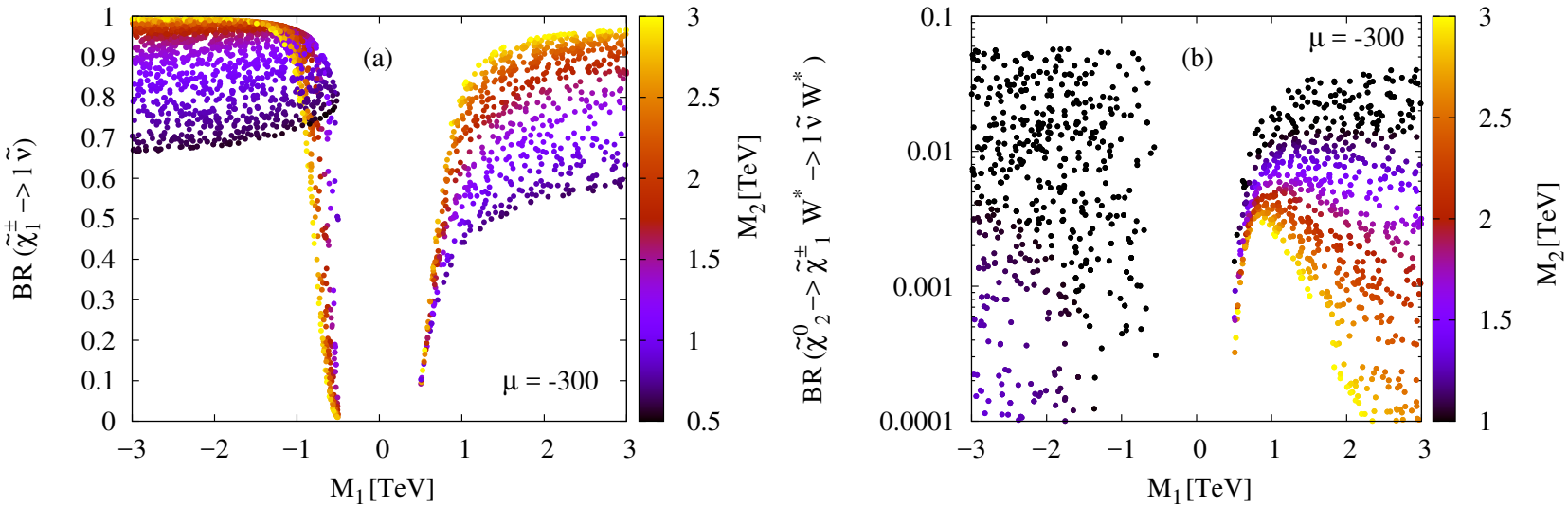

Figure : Variation of the leptonic branching ratios of $\widetilde{\chi}_1^{\pm} \to l\widetilde{\nu}$ and $\widetilde{\chi}_2^0 \to l\widetilde{\nu}W^*$ against the bino soft mass parameter, M_1 for the Higgsino mass parameter, $\mu = -300$ GeV. The wino mass parameter M_2 is indicated in the palette.